Journal of Applied Polymer Science

Synergistic Flame-Retardant Effect of Halloysite Nanotubes on Intumescent Flame Retardant in LDPE

Jing Zhao, Cheng-Liang Deng, Shuang-Lan Du, Li Chen, Cong Deng, Yu-Zhong Wang

Center for Degradable and Flame-Retardant Polymeric Materials, National Engineering Laboratory of Eco-Friendly Polymeric Materials (Sichuan), State Key Laboratory of Polymer Materials Engineering, College of Chemistry, Analytical and Testing Center, Sichuan University, Chengdu 610064, China

Correspondence to: Y. -Z. Wang (E-mail: yzwang@scu.edu.cn) or C. Deng (E-mail: dengcong@scu.edu.cn).

ABSTRACT: Synergistic flame-retardant effect of halloysite nanotubes (HNTs) on an intumescent flame retardant (IFR) in low-density polyethylene (LDPE) was investigated by limited oxygen index (LOI), vertical burning test (UL-94), thermogravimetric analysis (TGA), cone calorimeter (CC) test, and scanning electronic microscopy (SEM). The results of LOI and UL-94 tests indicated that the addition of HNTs could dramatically increase the LOI value of LDPE/IFR in the case that the mass ratio of HNTs to IFR was 2/28 at 30 wt % of total flame retardant. Moreover, in this case the prepared samples could pass the V-0 rating in UL-94 tests. CC tests results showed that, for LDPE/IFR, both the heat release rate and the total heat release significantly decreased because of the incorporation of 2 wt % of HNTs. SEM observations directly approved that HNTs could promote the formation of more continuous and compact intumescent char layer in LDPE/IFR. TGA results demonstrated that the residue of LDPE/IFR containing 2 wt % of HNTs was obviously more than that of LDPE/IFR at the same total flame retardant of 30 wt % at 700°C under an air atmosphere, and its maximum decomposing rate was also lower than that of LDPE/IFR, suggesting that HNTs facilitated the charring of LDPE/IFR and its thermal stability at high temperature in this case. Both TGA and SEM results interpreted the mechanism on the synergistic effect of HNTs on IFR in LDPE, which is that the migration of HNTs to the surface during the combustion process led to the formation of a more compact barrier, resulting in the promotion of flame retardancy of LDPE/IFR. In addition, the mechanical properties of LDPE/IFR/HNTs systems were studied, the results showed that the addition of 0.5–2 wt % of HNTs could increase the tensile strength and the elongation at break of LDPE/IFR simultaneously. © 2013 Wiley Periodicals, Inc. J. Appl. Polym. Sci. **2014**, *131*, 40065.

KEYWORDS: halloysite nanotube; intumescent flame retardant; synergistic effect; LDPE; clay; degradation; flame retardance; polyolefins; thermal properties

Received 8 May 2013; accepted 13 October 2013

DOI: 10.1002/app.40065

INTRODUCTION

As a result of the excellent physical properties, low-density polyethylene (LDPE) has been widely used in many fields, such as packaging materials, thin films, building materials, etc. However, its flammability and melt dripping restricted its applications in past several decades.[1–3] Therefore, it is very necessary to improve the flame retardancy of LDPE in order to expand its applications to more fields. Generally, several good methods can be used to enhance the flame retardancy of LDPE. The first one is to introduce halogen-containing flame retardant into LDPE. Generally, the high flame-retardant efficiency can be achieved via incorporating this category of flame retardant. However, halogen-containing flame retardants are being phased out for their proven or suspected adverse effects on the environment. The second one is to prepare the flame-retardant LDPE (FR-LDPE). Several prepared FR-LDPE have been obtained in past several decades. The last one is to add various halogen-free flame retardants into polymer matrix to promote its flame retardancy. At present, intumescent flame retardant (IFR) is deemed to be one of the most effective flame retardants to enhance the flame retardancy of LDPE because of its merits, such as its low loading, environmental friend, halogen-free, very low smoke, and toxic gases produced during burning.[4] The typical formulation of IFR consists of an acid source, a char forming agent and a blowing agent. During the combustion process, IFR forms an expanded charring layer at the burning surface, which can protect the matrix beneath from the heat flux or fire. The corresponding mechanism has been detailedly discussed by Camino et al.[5,6]

However, IFR has some drawbacks, for instance, low flame-retarded efficiency, and low thermal stability. To overcome the shortcomings of IFR, some works have been carried out, in which some synergistic agents, such as zeolites,[7] metallic compounds,[4,8–11] metal chelates,[12–14] and rare earth oxide,[15] were

incorporated into IFR to reinforce its flame-retarded efficiency and low thermal stability. In addition, some nanoparticles, especially layered silicates, have also been used to enhance the flame retardancy of polymer/IFR system. For example, Huang et al.[16] studied the synergistic effect between IFR and OMMT in LDPE matrix. Their results demonstrated that the addition of OMMT improved the thermal stability and significantly reduced the flammability. Generally, in order to improve the strength, thermal stabilities, and flame retardancy of polymer/layered silicate nanocomposites, the organic modification of nanoclays is very necessary to obtain the exfoliated or intercalated structures in the composites.[17,18] However, the modification process is quite complicated and costly. So it comes to be a hot subject to find the materials which do not need to be modified, but can meet the requirements of exfoliation and intercalation in composites.

As a kind of aluminosilicate clay ($Al_2Si_2O_5(OH)_4 \cdot 2H_2O$) with hollow nanotube structure,[19] the outer surface of HNTs is composed of siloxane, and its most of hydroxyls are located on the inner surface. Compared with other silicates, HNTs has less hydroxyl groups on the outer surface, several studies[20,21] have demonstrated that the dispersion of the clays with less hydroxyl groups on the outer surface might be better than those clays with more other hydroxyl groups at the same loading in nonpolar matrix. Generally, the better dispersion can endow polymer composite with better mechanical properties, higher thermal stability and better flame retardancy.[22–24] So HNTs should be an ideal material to enhance the thermal stability and flame retardancy of LDPE. Currently, some studies[25–28] have focused on polymer/HNTs nanocomposites to explore the contribution of HNTs to the thermal stability and flame retardancy of polymer matrix. Jia and coworkers[27] reported that the heat release rate and mass loss rate decreased because of the incorporation of a small amount of HNTs. In addition, the positive effect of HNTs on the mechanical properties of polymer was also investigated in previous work.[29–31] However, as a synergistic agent to enhance the flame retardancy and thermal stability of intumescent flame-retardant LDPE, there was seldom report.

In this work, HNTs was chosen as the synergistic agent to enhance the flame retardancy and thermal stability, and various measurements were used to analyze the synergistic efficiency of HNTs. In addition, the effect of HNTs on the mechanical properties of LDPE/IFR was also studied.

EXPERIMENTAL

Materials

LDPE (112A) and ammonium polyphosphate (APP-II, abbrev. APP) were purchased from Beijing Yanshan Petrochemical (China) and Shanghai Xusen (China), respectively. Charring agent (CA) named poly(1,3,5-triazin-2-aminoethanol) was provided by Weili Flame Retardant Chemicals, Chengdu, China. The untreated HNTs were supplied by Beijing Dibaohua Information Technology (Beijing, China). The lengths, outer diameters and inner diameters of HNTs are about 0.5–2 μm, 50–70 nm and 10–30 nm, respectively. The morphologies of untreated HNTs are shown in Figure 1.

Preparation of FR-LDPE Samples

IFR consisted of APP and CA, in which the ratio of APP/CA was 3/1, and the loadings of HNTs in LDPE/IFR were 0, 0.5, 1.0, 2.0, and 3.0 wt %, respectively. All the components were mixed via a high-speed mixer, and then the mixtures were extruded by a twin-screw extruder (CET 20, Kebeilong Keya, China) with the rotating speed of 100 rpm at the following temperature profile: 150°C, 160°C, 165°C, 170°C, 165°C, and 160°C from the feed zone to the die. The extrudates were cut into pellets. Finally, these pellets were hot-pressed into the standard samples according to the different requirements in various tests.

Figure 1. SEM micrograph of HNTs.

Measurements

Thermogravimetric analysis (TGA) was performed on a thermogravimetric analyzer instrument (209 F1, NETZSCH, Germany) at a heating rate of 10°C/min under air at a flow rate of 60 mL/min in the temperature range from 40 to 700°C.

Limiting oxygen index (LOI) values were surveyed on an oxygen index meter (HC-2C, Jiangning Analytical Instrument Factory, China) using the sheets with the dimensions of 130 mm × 6.5 mm × 3.2 mm according to ASTM D2863-97.

Vertical burning tests (UL-94) were measured on a vertical burning test instrument (CZF-2-type, Jiangning Analytical Instrument Factory, China) according to ASTM D3801.

Cone calorimeter (CC) tests were carried out by an FTT cone calorimeter (Fire Testing Technology, East Grinstead, UK), following the procedures described in ISO 5660-1. Each specimen (100 mm × 100 mm × 6 mm) was wrapped in aluminum and irradiated at a heat flux of 50 kW/m^2.

Scanning electronic microscopy (SEM) observations were performed by a FEI scanning electron microscope (Inspect F, FEI, USA) at an accelerating voltage of 10 kV to study the surface of char residues obtained from CC tests. All specimens were coated with a conductive layer before being examined.

Transmission electron micrographs (TEM) were obtained with an electron microscope (Tecnai G2 F20 S-TWIN, FEI, USA) at an accelerating voltage of 20 kV. Ultrathin specimens (approx. 50 nm) were prepared by ultramicrotomy at low temperature using a Leica EMUC6/FC6 low temperature sectioning system.

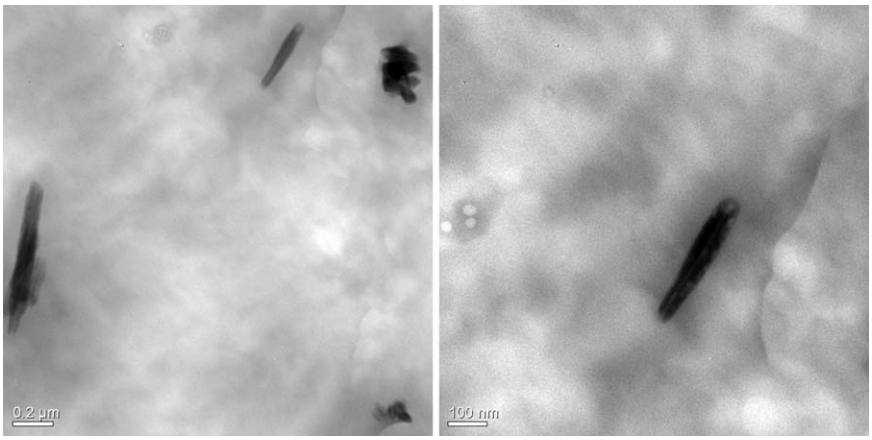

Figure 2. TEM micrographs of LDPE/IFR27/HNTs3.

Mechanical properties were tested on a universal experimental machine (CMT2000, SANS, Shenzhen, China) in accordance with the procedures in GB/T 1040- 1992 at an extension speed of 50 mm/min at room temperature. All data were the average of five independent measurements, and the standard errors were reported as well.

RESULTS AND DISCUSSION

Dispersion of HNTs in LDPE/IFR

The dispersion of nanoparticles in polymer matrix directly affects the mechanical properties, flame retardancy, and thermal stability of the matrix, so the dispersion of HNTs in FR-LDPE was investigated firstly through TEM. Generally, the dispersion of HNTs has no great change at low loading, so we selected the LDPE/IFR27/HNTs3 sample to confirm the dispersion of HNTs. The TEM micrographs (Figure 2) reveal that HNTs dispersed well in polymer matrix, suggesting that the addition of HNTs might contribute to the improvement of comprehensive performance of LDPE/IFR.

Flame Retardancy

To investigate the synergistic effect of HNTs on IFR in preparing FR-LDPE, the LOI and UL-94 tests were performed for various LDPE systems. The corresponding results are shown in Table I. Here, it should be noted that the total loading of flame retardant is 30 wt % for all systems. With the incorporation of 30 wt % of IFR, the LOI value of FR-LDPE increases to 29 from 17 for neat LDPE, and the UL-94 classification of FR-LDPE also goes up to the V-0 rating from no rating for neat LDPE. With the addition of HNTs, the LOI value further increases, and it reaches the maximum value of 36.5 when the content of HNTs is 2.0 wt %, and then it decreases with the incorporation of more HNTs. The LOI value reduces to 35.0 at the loading of 3.0 wt % of HNTs. However, the UL-94 rating for FR-LDPE at 3.0 wt % of HNTs still keeps the V-0 rating.

Table I. Effect of HNTs on the Flame Retardancy of LDPE/IFR

LDPE (%)	IFR (%)	HNTs (%)	LOI (%)	UL-94 (3.2 mm)
100	0	0	17.0 ± 0.5	N.R.
70	30.0	0	29.0 ± 0.3	V-0
70	29.5	0.5	32.7 ± 0.4	V-0
70	29.0	1.0	33.1 ± 0.3	V-0
70	28.0	2.0	36.5 ± 0.2	V-0
70	27.0	3.0	35.0 ± 0.5	V-0

Based on the results mentioned above, the weight ratio of 2/28 for HNTs/IFR was chosen as the constant value in the following investigation concerning the effect of the loading of compounded flame retardant consisting of IFR and HNTs on the flame retardancy of LDPE. The total loadings of IFR/HNTs in LDPE are 30, 27.5, 25, 22.5, and 20 wt %, respectively. The experimental results are shown in Table II. With decreasing the compounded flame retardant, the LOI value of LDPE/IFR/HNTs goes down. The LOI value decreases to 23.1 at 20 wt % of IFR/HNTs from 36.5 at 30 wt % of IFR/HNTs. All the UL-94 ratings of LDPE/IFR/HNTs samples are V-0 when the content of IFR/HNTs is in the range of 25–30 wt %, whereas the UL-94 rating is no rating below 25 wt % of IFR/HNTs. According to the results mentioned above, the lowest content of IFR/HNTs in LDPE is about 25 wt % to achieve the V-0 rating in UL-94 test.

Combustion Performance

CC test based on the oxygen consumption is one of the most effective methods to evaluate a flame retardant. The combustion in CC test is similar to that occurred in a real incident, so the CC test result can efficiently reflect the fire performance of the prepared sample. In order to investigate the synergistic effect of HNTs on IFR in LDPE during the combustion process, CC tests were performed in this study. The fire performances for LDPE

Table II. Effect of the Content of IFR/HNTs on the Flame Retardancy of LDPE/IFR

LDPE (%)	IFR/HNTs (%)	LOI (%)	UL-94 (3.2 mm)
70.0	30.0	36.5 ± 0.2	V-0
72.5	27.5	30.5 ± 0.5	V-0
75.0	25.0	29.9 ± 0.3	V-0
77.5	22.5	27.6 ± 0.5	N.R.
80.0	20.0	23.1 ± 0.6	N.R.

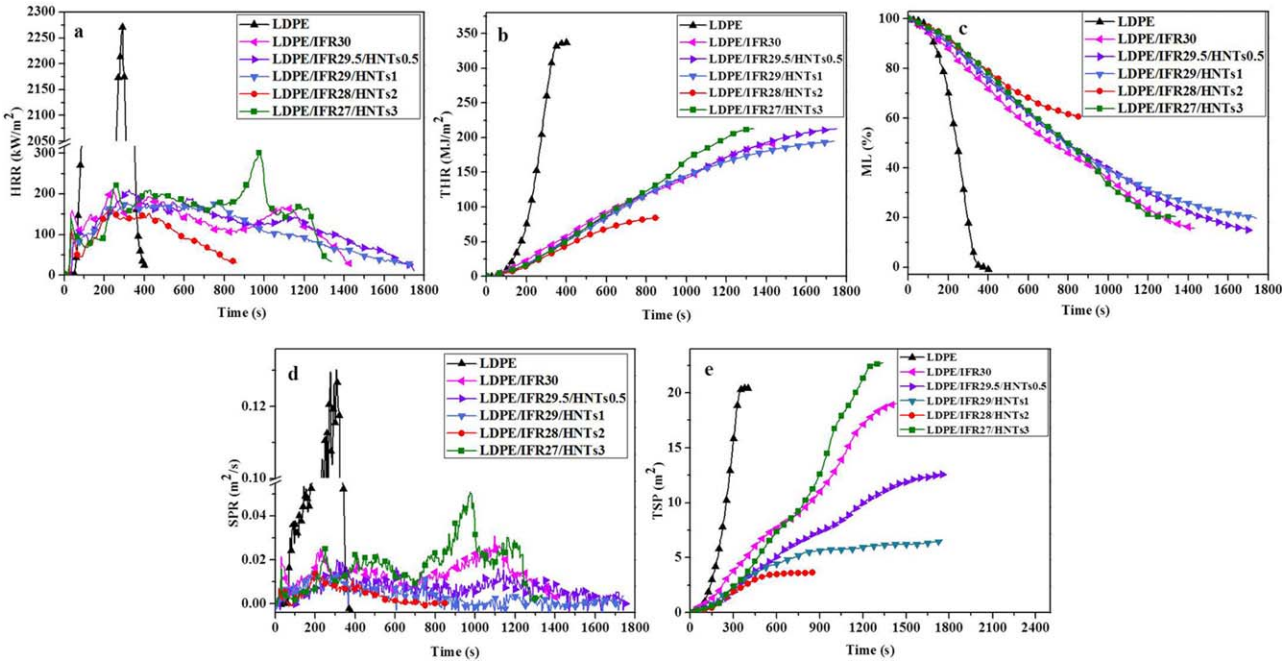

Figure 3. CC tests results: (a) HRR, (b) THR, (c) ML, (d) SPR, and (e) TSP. [Color figure can be viewed in the online issue, which is available at wileyonlinelibrary.com.]

and FR-LDPE composites are shown in Figure 3 and Table III, including the heat release rate (HRR), total heat release (THR), mass loss (ML), smoke produce rate (SPR), total smoke production (TSP), and time to ignition (TTI).

Figure 3(a) shows the HRR curves of neat LDPE and FR-LDPE samples. It can be seen that the peak of heat release rate (pHRR) is 2271 kW/m^2 for neat LDPE; whereas the pHRR value for FR-LDPE system is apparently lower than that of neat LDPE. Moreover, with the addition of HNTs the pHRR further decreases to 162 kW/m^2 for LDPE/IFR28/HNTs2 from 210 kW/m^2 for LDPE/IFR. However, it goes up to 219 kW/m^2 with increasing the HNTs up to 3 wt %. Generally, the decrease of HRR values implies that the tested material has higher fire safety. So these results suggest that LDPE/IFR28/HNTs2 system has the highest fire safety among these materials presented in Figure 3(**a**).

It is well-known that higher THR value means that there is more heat release during buring, and the higher THR may result in dangerous secondary fire. An obvious THR decrease was observed for LDPE containing IFR compared with neat LDPE. Figure 3(b) shows that the THR of neat LDPE is 337 MJ/m^2. Compared with neat LDPE, the THR is reduced by 43, and 75% for LDPE/IFR30, and LDPE/IFR28/HNTs2, respectively. Obviously, HNTs decreased the THR of LDPE/IFR very efficiently in CC tests. Accordingly, the possibility of dangerous secondary fire may apparently decrease because of the presence of HNTs in LDPE/IFR. Especially at the loading of 2 wt % of HNTs, the THR is lowest, meaning that it is the most efficient to reduce the secondary fire at about the content of 2 wt % for LDPE/IFR/HNTs system.

Figure 3(c) shows the ML curves of neat LDPE and FR-LDPE systems as a function of combustion time. After the combustion, nothing was left for neat LDPE, whereas the char residues for LDPE/IFR30, LDPE/IFR29.5/HNTs0.5, LDPE/IFR29/HNTs1, LDPE/IFR28/HNTs2, and LDPE//IFR27/HNTs3 were 15.7, 15.1, 19.8, 60.6, and 20.4 wt %, respectively. Generally, the more char residue can decrease the produce of combustible gases during the combustion process, and can also prevent the mass and heat transfer, consequently improve the flame retardancy of materials[32]. The ML test indicated that the char residue gradually

Table III. The Data Obtained from CC Tests for all LDPE Systems

Sample	TTI(s)	pHRR (kW/m^2)	T_{pHRR}(s)	THR(MJ/m^2)	Residue(%)	pSPR($\times10^{-2}$m^2/s)	TSP(m^2)
LDPE	49	2271	290	337	0	12.9	20.5
LDPE/IFR30	22	210	240	191	15.7	2.7	19.0
LDPE/IFR29.5/HNTs0.5	22	209	325	212	15.1	2.0	12.6
LDPE/IFR29/HNTs1	18	182	310	194	19.8	1.5	6.5
LDPE/IFR28/HNTs2	21	162	225	85	60.6	1.4	3.6
LDPE/IFR27/HNTs3	19	219	250	213	20.4	5.1	22.7

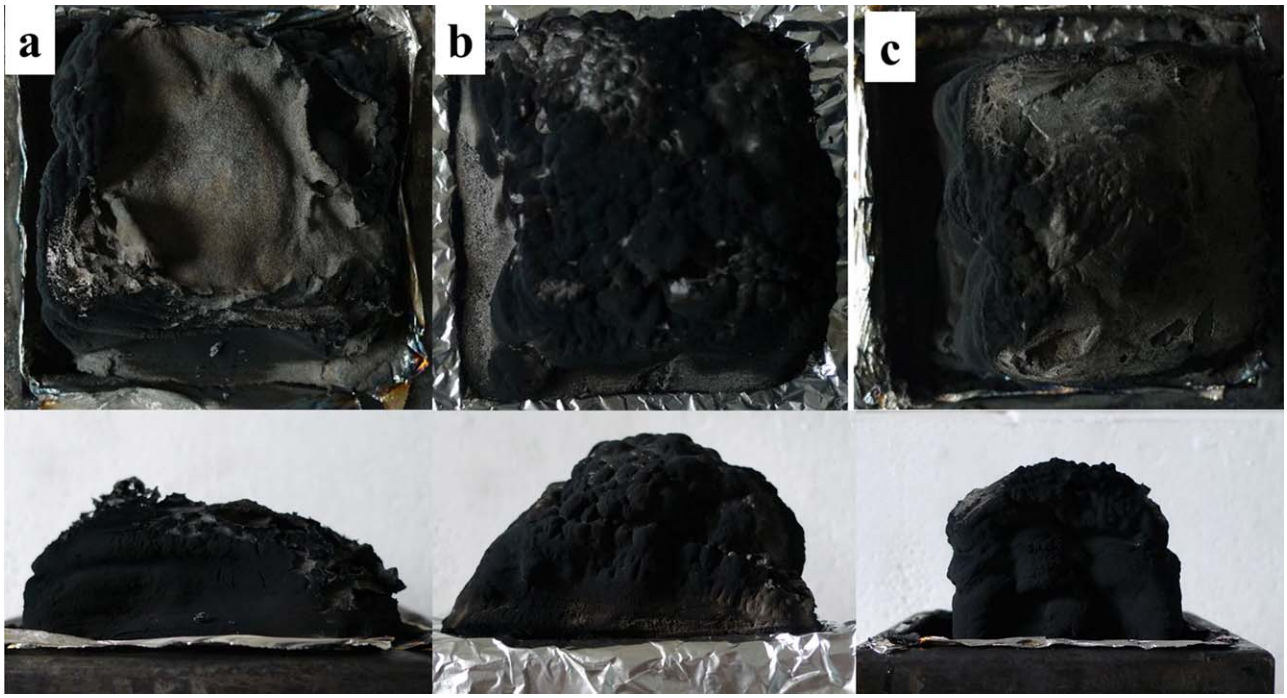

Figure 4. Digital photographs of residual chars after cone test, (a) LDPE/IFR30, (b) LDPE/IFR28/HNTs2, and (c) LDPE/IFR27/HNTs3. [Color figure can be viewed in the online issue, which is available at wileyonlinelibrary.com.]

increased with the addition of HNTs, and it reached the maximum value (60.6 wt %) when the content of HNTs was 2 wt %. With further increasing the HNTs to 3 wt %, the char residue decreased significantly to 20.4 wt %. Generally, more char residue may contribute to the formation of more continuous and more compact char layer which can better inhibit the loss of the flammable gases and better protect the unburned matrix from the heat flux, so the FR-LDPE containing 2 wt % of HNTs might have better flame retardancy than other FR-LDPE systems.

The lower smoke production also plays an important role in reducing the fire danger. Figure 3(d,e) show the SPR and TSP curves of LDPE and FR-LDPE. As can be seen in Figure 3(d), the SPR peak (pSPR) values of LDPE/IFR30, LDPE/IFR29.5/HNTs0.5, LDPE/IFR29/HNTs1, and LDPE/IFR28/HNTs2 are much lower than that of neat LDPE (0.129), and they are 0.027, 0.020, 0.015, and 0.014 m^2/s, respectively; whereas the pSPR of LDPE/IFR27/HNTs3 increases to 0.051, which is also much lower than that of neat LDPE. Figure 3(e) indicates that, compared to neat LDPE, TSP decreases from 20.5 to 19.0, 12.6, 6.5, and 3.6 m^2 for LDPE/IFR30, LDPE/IFR29.5/HNTs0.5, LDPE/IFR29/HNTs1, and LDPE/IFR28/HNTs2, respectively; whereas the TSP increases to 22.7 m^2 at the loading of 3 wt % of HNTs, which is higher than that of LDPE. Based on the results mentioned above, it can be concluded that the incorporation of HNTs may contribute to improve the performance of smoke production for FR-LDPE system. Moreover, the synergistic effect is best at about 2 wt % of HNTs in the range investigated.

The TTI values of all the FR-LDPE systems are lower than that of neat LDPE, the value reduces to about 20 s from 49 s with the addition of IFR and HNTs. The reason might be the increase of heat flux as the swollen layer approached the cone heater, or the flame retardants played their roles.[33]

SEM Observation

The morphology of the formed char after combustion could supply direct evidence to evaluate the flame-retardant efficiency of flame retardant. Figure 4 presents the digital photos of residual chars for LDPE/IFR30, LDPE/IFR28/HNTs2, and LDPE/IFR27/HNTs3 after CC tests. All the char layers of these samples are typically intumescent state. Obviously, in terms of the degree of expansion, that of LDPE/IFR28/HNTs2 is higher than those of LDPE/IFR30 and LDPE/IFR27/HNTs3. In order to obtain more detailed information on the residual chars, SEM measurements were performed after CC tests. Figure 5(a) shows that the chars of LDPE/IFR30 are quite loose, and there are many holes at the outer and inner surfaces of the residual chars. For LDPE/IFR28/HNTs2, the outer and inner surfaces are more homogenous and more compact [Figure 5(b1,b3)] than those of LDPE/IFR30, and only a few holes can be observed at the two surfaces. In addition, Figure 5(b2) shows that there are many tubular-like structures at the outer surface for LDPE/IFR28/HNTs2, which might result from the migration of HNTs to the surface during the burning,[34,35] moreover, the dimensions of these tubular-like structures are bigger than those of natural HNTs shown in Figure 1, which might be owe to the clustering of residue chars on the surfaces of HNTs.[36] Through the combination of digital photos and SEM micrographs, it can be demonstrated that one of the reasons for the higher flame-retardant efficiency at about 2 wt % of HNTs might be ascribed to the

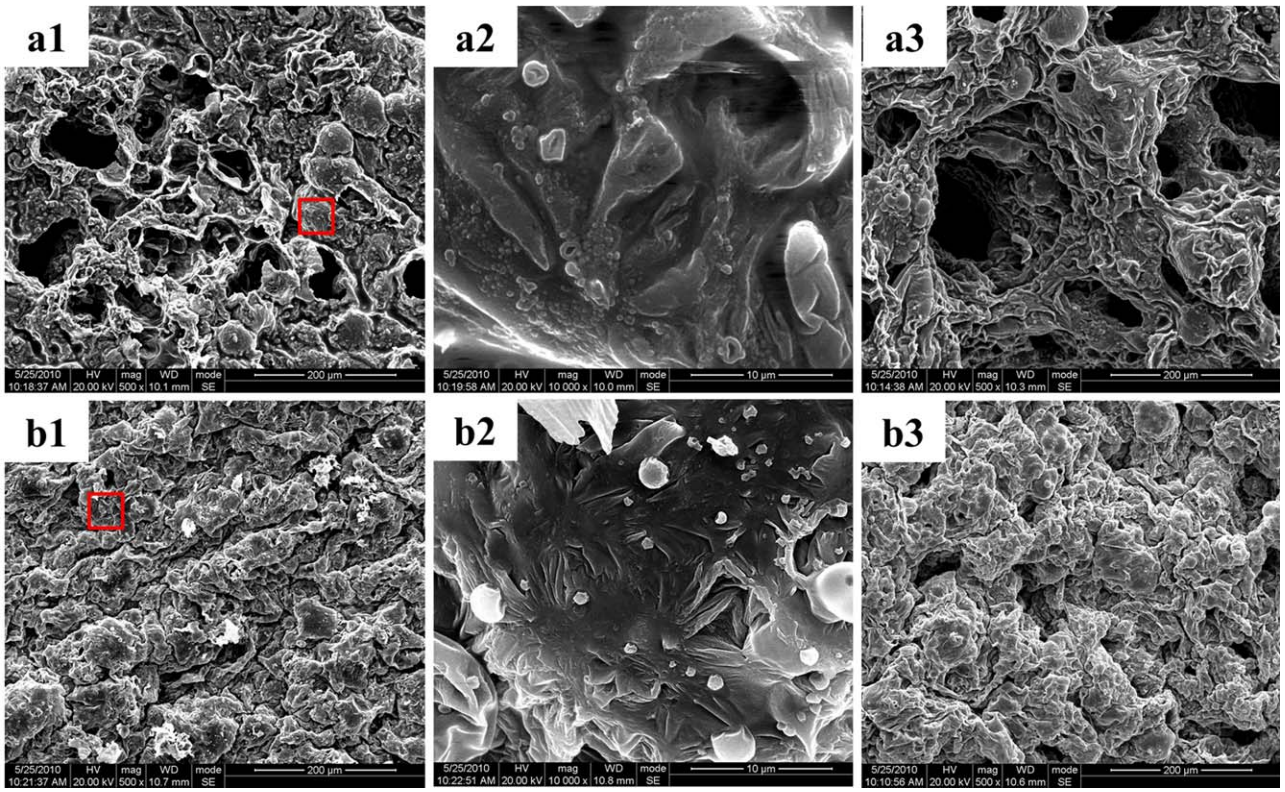

Figure 5. SEM photographs of the outer and inner surfaces of intumescent chars obtained from cone tests: LDPE/IFR30 (a1, outer × 500; a2, outer × 10,000; a3, inner × 500), LDPE/IFR28/HNTs2 (b1, outer × 500; b2, outer × 10,000; b3, inner × 500). [Color figure can be viewed in the online issue, which is available at wileyonlinelibrary.com.]

higher degree of expansion, more compact char layer, and the migration of HNTs.

Thermal Decomposing Behavior

TGA curves of neat LDPE and FR-LDPE systems under an air atmosphere are plotted in Figure 6(a), and their corresponding DTG curves are shown in Figure 6(b). $T_{5\%}$ (the temperature at 5 wt % of mass loss), T_{max} (the temperature at maximum decomposition rate), and the residues of all samples are summarized in Table IV. For neat LDPE, the value of $T_{5\%}$ is about 261°C, and the values of T_{max1} and T_{max2} are 298.8°C and 395.6°C, respectively. In addition, the amount of char residue is almost zero after the combustion. With the incorporation of 30 wt % IFR, the $T_{5\%}$, T_{max1}, and T_{max2} were greatly affected, and gave 4.7 wt % char residue at 700°C. For LDPE/IFR28/HNTs2, its $T_{5\%}$, T_{max1}, and T_{max2} increase to 334, 409.5, and 442.0°C,

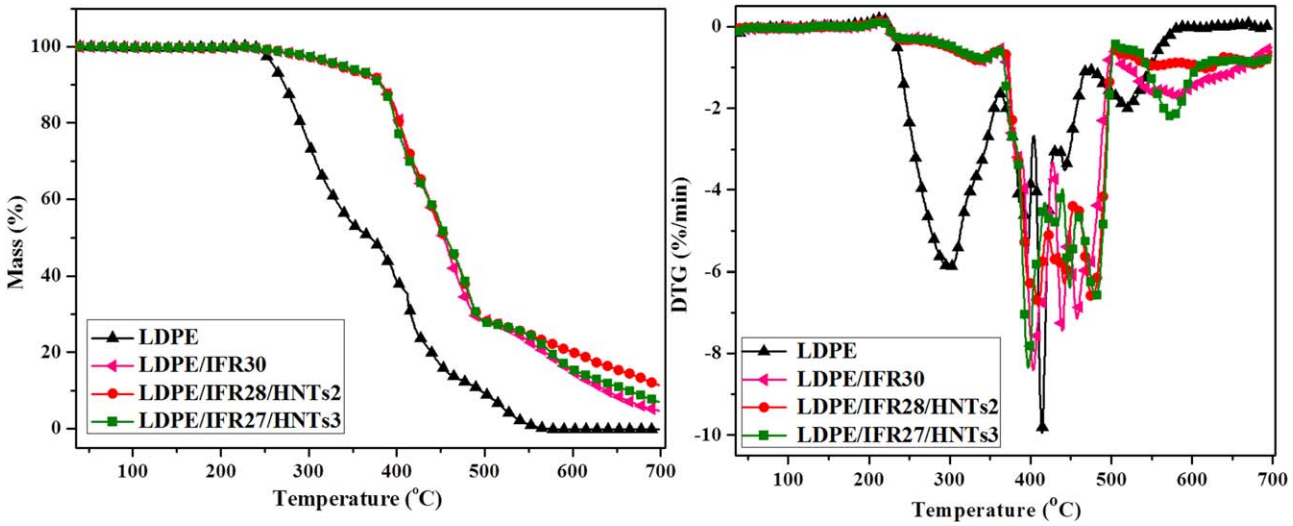

Figure 6. TGA curves of LDPE and FR-LDPE systems. (a) TGA and (b) DTG. [Color figure can be viewed in the online issue, which is available at wileyonlinelibrary.com.]

Table IV. TGA Data of LDPE and FR-LDPE Systems

Sample	$T_{5\%}$ (°C)	T_{max1} (°C)	T_{max2} (°C)	The decomposing rate at T_{max} (wt %/min)	Char residue (wt %) 700°C
LDPE	261	298.8	395.6	15.69	0
LDPE/IFR30	336	403.2	439.1	8.41	4.7
LDPE/IFR28/HNTs2	334	409.5	442.0	6.79	11.5
LDPE/IFR27/HNTs3	338	397.1	448.7	8.36	7.0

respectively. Moreover, the maximum char residue is 11.5 wt % at 700°C. TGA data illustrate that the decomposing rate for FR-LDPE was influenced by HNTs at high temperature. Table IV shows that the decomposing rate is 8.41 wt %/min when the content of IFR is 30 wt %. With the incorporation of 2 wt % of HNTs, it decreases to 6.79 wt %/min. With further increasing the HNTs up to 3 wt %, the decomposing rate does not decrease, but increase to 8.36 wt %/min. In addition, the char residue decreases to 7.0 wt % at 700°C in this case. These results demonstrate that HNTs have an effect on the thermal stability of IFR, and the impact is related to the content of HNTs.

Synergistic Flame-Retardant Mechanism

TGA is one of the effective methods to investigate the flame-retardant mechanism.[37] In order to interpret the synergistic flame-retardant mechanism between IFR and HNTs, the IFR and IFR/HNTs systems were analyzed by TGA under a nitrogen atmosphere. The results are presented in Figure 7 and Table V. Here, the corresponding fitted curve was obtained based on the hypothesis that there was no reaction between any two components. For DTG results of IFR and IFR28/HNTs2, there are three mass loss peaks that should be assigned to the releases of water and ammonia, the decomposition and char-forming of IFR, and the decomposition of char residues, respectively.[38] For IFR/HNTs, the fitted value of ML is much higher than the real one, suggesting that HNTs facilitated the formation of char residue. In DTG results of IFR28/HNTs2, the fitted T_{max1} and T_{max2} have no great change in comparison with the experimental values, meaning that the former two processes were not greatly affected by the incorporation of HNTs. However, the real experimental T_{max3} is 587.0°C that is much higher than that of the fitted one, suggesting that the decomposition of char residue was delayed because of the presence of HNTs in IFR/HNTs. According to Lewin M's viewpoint,[34] the migration of HNTs to the surface should be the leading effect to the improvement of flame retardancy in LDPE/IFR system. Here, only the real experimental T_{max3} increases with the incorporation of HNTs, meaning that HNTs mainly militated at the last decomposing process (the decomposition of char residues). Based on the tests results, the synergistic flame-retardant mechanism of HNTs in this experiment can be concluded as follows. Upon heating, HNTs gradually migrated to the surface of burning samples, and then engaged in the formation of char layer, leading the formation of a protective barrier containing some HNTs. During the releases of water and ammonia, and the decomposition and char-forming of IFR, the thermal stability of sample was scarcely affected by the presence of some HNTs. With the aggregation of more and more HNTs at the surface of burning samples, the protective barrier began to greatly affect the flame retardancy of LDPE, finally delayed the decomposition of char residue at high temperature.

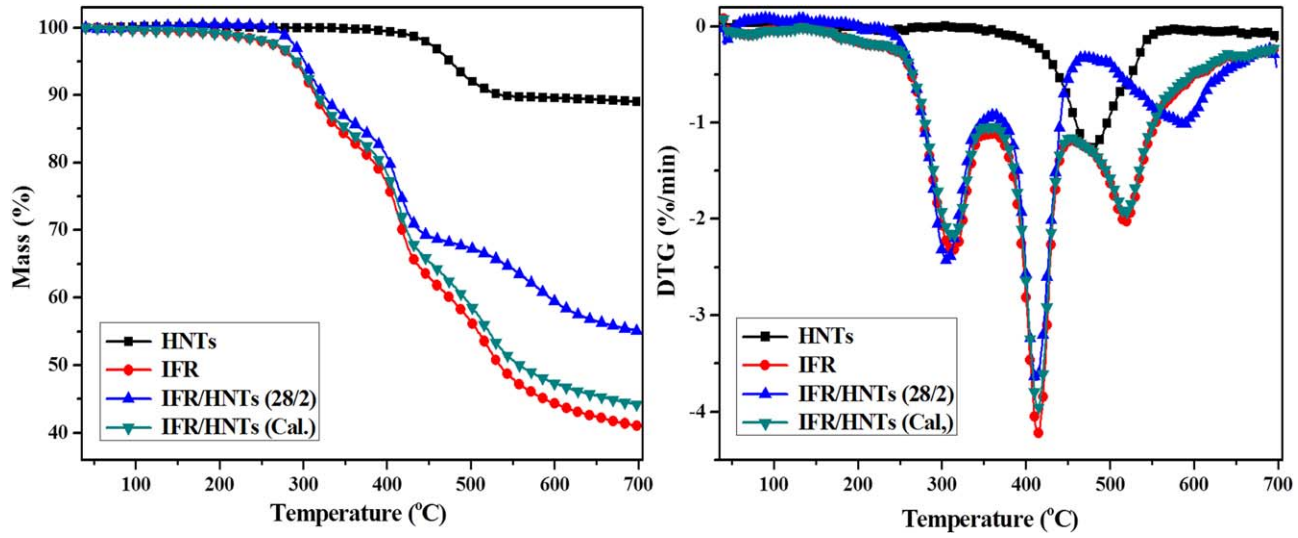

Figure 7. TGA and DTG curves of IFR, IFR/HNTs and IFR/HNTs(Cal.). (a) TGA and (b) DTG. [Color figure can be viewed in the online issue, which is available at wileyonlinelibrary.com.]

Table V. TGA Data of IFR, IFR/HNTs and IFR/HNTs(Cal.)

Sample	$T_{5\%}$(°C)	T_{max1}(°C)	T_{max2}(°C)	T_{max3}(°C)	Char residue (wt %)700°C
HNTs	475.4	473.5	-	-	89.0
IFR[a]	288.6	296.1	411.8	513.6	41.1
IFR/HNTs [b](28/2)	301.0	305.9	412.1	587.0	55.1
IFR/HNTs [c](Cal.)	292.0	314.0	414.0	544.0	44.2

[a] IFR is composed of APP and CA, and the ratio of APP/CA is 3/1.
[b] The mass ratio of IFR/HNTs is 28/2.
[c] $W_{cal} = W_{IFR} \times 93.33\ \% + W_{HNTs} \times 6.67\ \%$.

Tensile Property

The tensile properties of LDPE/IFR30 and LDPE/IFR/HNTs systems are listed in Table VI. It can be seen that the tensile strength (δ) of LDPE/IFR increases in the presence of 0.5–2 wt % HNTs compared with neat LDPE, and the elongation at break (ε) also increases in this range. However, when the content of HNTs is 3 wt %, only is the tensile strength enhanced, whereas the elongation at break decreases. The improvement of tensile property might result from the good dispersion of HNTs in LDPE/IFR. TEM micrographs have confirmed that HNTs dispersed well in polymer matrix. Overall, both the tensile strength and the elongation at break of LDPE/IFR can be improved at low loading of HNTs. Combined with the flame retardancy of LDPE/IFR/HNTs, it can be concluded that not only can the flame retardancy of LDPE/IFR be promoted in the presence of a small amount of HNTs, but also its tensile property may also be increased in this case.

CONCLUSIONS

The flame-retardant effect of HNTs on IFR in LDPE was investigated by different measurements. The results of LOI, UL-94, and CC tests indicated that the addition of 2 wt % of HNTs into LDPE/IFR improved the flame retardancy of LDPE/IFR. The UL-94 classification was V-0 rating at the content of HNTs was 2 wt %, and the LOI value reached 36.5. In addition, the HRR, THR, pHRR, SPR, TSR, and TTI significantly decreased because of the incorporation of 2 wt % of HNTs, whereas the char residue at this loading apparently increased compared with neat LDPE. The morphological structures of the inner and outer char residues directly illustrated that the addition of HNTs into LDPE/IFR led to the formation of more compact char layers. TGA results combined with SEM results further revealed the following synergistic flame-retardant mechanism. HNTs migrated to the surface of burning samples upon heating, and then engaged in the formation of more compact char layer, consequently resulting in the enhancement of the flame retardancy of LDPE/IFR. Furthermore, the tensile property of LDPE/IFR was also enhanced in the presence of a small amount of HNTs.

Table VI. Effect of the Content of HNTs on the Tensile Property of LDPE/IFR/HNTs

LDPE (%)	IFR (%)	HNTs (%)	δ (MPa)	ε (%)
70.0	30.0	0	8.47 ± 0.3	66.49 ± 10
70.0	29.5	0.5	9.30 ± 0.2	73.18 ± 15
70.0	29.0	1.0	9.73 ± 0.3	69.20 ± 20
70.0	28.0	2.0	9.61 ± 0.5	68.47 ± 5
70.0	27.5	3.0	9.92 ± 0.4	62.02 ± 20

ACKNOWLEDGMENTS

We gratefully acknowledge support from the Natural Science Foundation of China (Grant Nos. 50933005 and 51121001) and the Program for Changjiang Scholars and Innovative Research Teams in University of China (IRT 1026).

REFERENCES

1. Wu, Z. P.; Shu, W. Y.; Hu, Y. C. *J. Appl. Polym. Sci.* **2007**, *103*, 3667.
2. Ravadits, I.; Toth, A.; Marosi, G.; Marton, A.; Szep, A. *Polym. Degrad. Stab.* **2001**, *74*, 419.
3. Liu, Y.; Wang, D. Y.; Wang, J. S.; Song, Y. P.; Wang, Y. Z. *Polym. Adv. Technol.* **2008**, *19*, 1566.
4. Nie, S. B.; Song, L.; Tai, Q. L.; Zhan, J.; Lu, H. D.; Hu, Y. *Polym. Plast. Technol. Eng.* **2009**, *48*, 464.
5. Camino, G.; Costa, L.; Martinasso, G. *Polym. Degrad. Stab.* **1989**, *23*, 359.
6. Horacek, H.; Grabner, R. *Polym. Degrad. Stab.* **1996**, *54*, 205.
7. Demir, H.; Arkış, E.; Balköse, D.; Ülkü, S. *Polym. Degrad. Stab.* **2005**, *89*, 478.
8. Chen, X. C.; Ding, Y. P.; Tang, T. *Polym. Int.* **2005**, *54*, 904.
9. Cullis, C. F.; Hirschler, M. M.; Thevaranjan, T. R. *Eur. Polym. J.* **1984**, *20*, 841.
10. Gallo, E.; Schartel, B.; Braun, U.; Russo, P.; Acierno, D. *Polym. Adv. Technol.* **2011**, *22*, 2382.
11. Song, R. J.; Zhang, B. Y.; Huang, B. Y.; Tang, T. *J. Appl. Polym. Sci.* **2006**, *102*, 5988.
12. Wang, D. Y.; Liu, Y.; Ge, X. G.; Wang, Y. Z.; Stec, A.; Biswas, B.; Hull, T. R.; Price, D. *Polym. Degrad. Stab.* **2008**, *93*, 1024.
13. Wang, D. Y.; Liu, Y.; Wang, Y. Z.; Artiles, C. P.; Hull, T. R.; Price, D. *Polym. Degrad. Stab.* **2007**, *92*, 1592.
14. Wang, D. L.; Liu, Y.; Wang, D. Y.; Zhao, C. X.; Mou, Y. R.; Wang, Y. Z. *Polym. Degrad. Stab.* **2007**, *92*, 1555.
15. Li, Y. T.; Li, B.; Dai, J. F.; Jia, H.; Gao, S. L. *Polym. Degrad. Stab.* **2008**, *93*, 9.

16. Huang, G. B.; Zhu, B. C.; Shi, H. B. *J. Appl. Polym. Sci.* **2011**, *121*, 1285.
17. Alexandre, M.; Dubois, P. *Mater. Sci. Eng. R.* **2000**, *28*, 1.
18. Song, R. J.; Wang, Z.; Meng, X. Y.; Zhang, B. Y.; Tang, T. *J. Appl. Polym. Sci.* **2007**, *106*, 3488.
19. Joussein, E.; Petit, S.; Churchman, J.; Theng, B.; Righi, D.; Delvaux, B. *Clay Miner.* **2005**, *40*, 383.
20. Tjong, S. C. *Mater. Sci. Eng. R* **2006**, *53*, 73.
21. Beatrice, C. A. G.; Branciforti, M. C.; Alves, R. M. V.; Bretas, R. E. S. *J. Appl. Polym. Sci.* **2010**, *116*, 3581.
22. Alamri, H.; Low, I. M. *Polym. Compos.* **2012**, *33*, 589.
23. Liu, C.; Luo, Y. F.; Jia, Z. X.; Zhong, B. C.; Li, S. Q.; Guo, B. C.; Jia, D. M. *Int. J. Polym. Mater. Polym. Biomater.* **2012**, *62*, 128.
24. Marney, D. C. O.; Russell, L. J.; Wu, D. Y.; Nguyen, T.; Cram, D.; Rigopoulos, N.; Wright, N.; Greaves, M. *Polym. Degrad. Stab.* **2008**, *93*, 1971.
25. Du, M. L.; Guo, B. C.; Jia, D. M. *Polym. Int.* **2010**, *59*, 574.
26. Pasbakhsh, P.; Ismail, H.; Fauzi, M. N. A.; Bakar, A. A. *Polym. Test.* **2009**, *28*, 548.
27. Jia, Z. X.; Luo, Y. F.; Guo, B. C.; Yang, B. T.; Du, M. L.; Jia, D. M. *Polym. Plast. Technol. Eng.* **2009**, *48*, 607.
28. Prashantha, K.; Lacrampe, M. F.; Krawczak, P. *Express Polym. Lett.* **2011**, *5*, 295.
29. Liu, M. X.; Guo, B. C.; Du, M. L.; Chen, F.; Jia, D. M. *Polymer* **2009**, *50*, 3022.
30. Liu, M. X.; Guo, B. C.; Zou, Q. L.; Du, M. L.; Jia, D. M. *Nanotechnology* **2008**, *19*, 205709.
31. Liu, M. X.; Jia, Z. X.; Liu, F.; Jia, D. M.; Guo, B. C. *J. Colloid Interf. Sci.* **2010**, *350*, 186.
32. Qin, H. L.; Zhang, S. M.; Zhao, C. G.; Hu, G. J.; Yang, M. S. *Polymer* **2005**, *46*, 8386.
33. Gallina, G.; Bravin, E.; Badalucco, C.; Audisio, G.; Armanini, M.; De Chirico, A.; Provasoli, F. *Fire Mater.* **1998**, *22*, 15.
34. Lewin, M.; Pearce, E. M.; Levon, K.; Mey-Marom, A.; Zammarano, M.; Wilkie, C. A.; Jang, B. N. *Polym. Adv. Technol.* **2006**, *17*, 226.
35. Tang, Y.; Lewin, M. *Polym. Degrad. Stab.* **2007**, *92*, 53.
36. Liu, Y.; Deng, C. L.; Zhao, J.; Wang, J. S.; Chen, L.; Wang, Y. Z. *Polym. Degrad. Stab.* **2011**, *96*, 363.
37. Duquesne, S.; Delobel, R.; Le Bras, M.; Camino, G. *Polym. Degrad. Stab.* **2002**, *77*, 333.
38. Li, B.; Xu, M. *J. Polym. Degrad. Stab.* **2006**, *91*, 1380.